Materials Research Proceedings **32** (2023) 264-273 https://doi.org/10.21741/9781644902615-30

Comparative studies of hyperbolic sine constitutive models for constant pressure superplastic tests

Luis García-Barrachina[1,a,*] and Antonio J. Gámez[1,b]

[1]School of Engineering, University of Cadiz, Av. Universidad de Cadiz, 10, E-11519 Puerto Real (Cadiz), Spain

[a]luis.barrachina@uca.es, [b]antoniojuan.gamez@uca.es

Keywords: Modelling, Constitutive Parameters, Hyperbolic Sine Model, Free-Inflation Test

Abstract. The constant pressure free-inflation test is a very versatile and simple tool for analyzing different features of superplastic forming. In recent years, different methods have been proposed to measure constitutive parameters of the stress–strain relationship for the superplastic material, specifically the *K* and *m* parameters of the power law model. However, this law is restricted to be used in narrow strain-rate ranges, and poor results are obtained when applied in a broader spectrum. To overcome this problem, numerous constitutive models covering the full strain-rate range applicable in superplastic forming have been proposed historically, including the hyperbolic sine equation. However, there is no clear consensus on the type of hyperbolic sine function to use. Some authors include a sensitivity parameter while others do not. This article aims to study the characteristics of the hyperbolic sine constitutive model, checking which of the historically proposed models achieves better results in the test at free deformation and constant pressure.

Introduction

It is well known the multi-variable complexity of the superplastic behavior and its dependency on so many factors, such as temperature, microstructure, deformation, strain rate or degradation of the material itself [1]. This makes modelling a complex task and continuous studies are carried out to improve the accuracy and consistency [2–4].

The behavior of a material in its superplastic regime can be extracted, as is usual, from tensile tests where the sample is subjected to a constant strain rate and the stress versus strain is contrasted [5]. Thus, the flow stress dependence of the strain rate is normally characterized by the sensitivity index *m*.

$$m = \frac{\partial \log \sigma}{\partial \log \dot{\varepsilon}} \tag{1}$$

This is taken as a parameter (between 0.3 and 0.7) for the quality of the superplastic behavior, providing shorter forming times and smaller final thickness gradients for higher values [6]. Thus, it is also common to express the behavior of the material as a flow stress function of the strain rate. Where the parameter *m* is related as the slope in the logarithmic variant of this graph. So it can be expressed as a potential law adding two material constants (*K, m*)

$$\sigma = K\dot{\varepsilon}^m \tag{2}$$

Alternatively, the importance of *m* can be understood changing (2) by introducing an apparent viscosity variable μ_a [7], such as

Materials Research Proceedings **32** (2023) 264-273 https://doi.org/10.21741/9781644902615-30

$$\sigma = \mu_a \dot{\varepsilon} \tag{3}$$

Thus, it is straightforward to associate the behavior of the material and its strain-rate dependence with the apparent viscosity variable

$$\mu_a = K\dot{\varepsilon}^{m-1} \tag{4}$$

such that if it is plotted versus the strain rate, Fig. 1, it is observed that the higher the value of *m*, the more homogeneous the behavior in the strain-rate range.

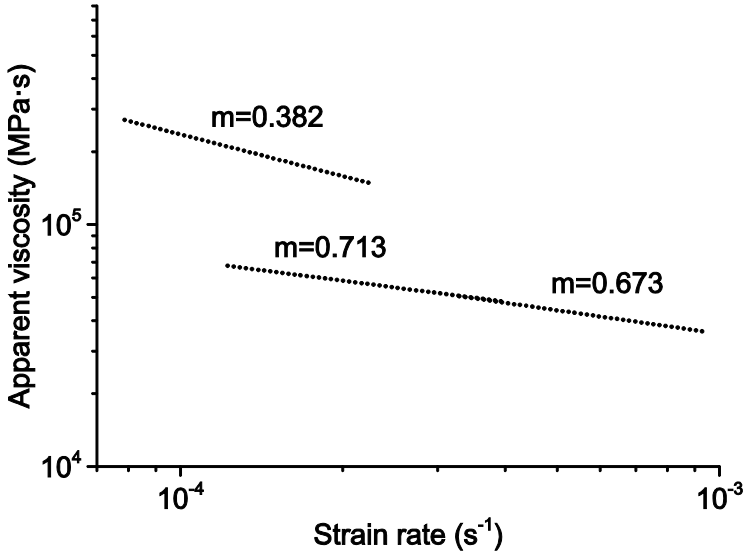

Fig 1. Effect of the m parameter on the apparent viscosity material variable. A higher value of m provides a more homogeneous behavior in the strain-rate range. Values for a titanium alloy at 800 (m=0.328) and 850 ºC (m=0.713 and m=0.673)

However, as it was previously mentioned, the material is highly dependent on the strain rate. Thus, the ability to model the behavior of the material through a constant-parameter potential equation is only valid for a given range of strain rate, where the behavior can be fitted to a straight line on the logarithmic scale. As the constitutive equation moves away from the actual behavior of the material, the ability to replicate real examples in computational models is reduced, increasing the discrepancy between the two.

In order to match the material behavior over a wider strain-rate range, different constitutive models have historically been proposed: polynomial forms [8], unified constitutive equations including microstructure evolution models [2,9] or anisotropy plus grain size models [10]. [11] can be consulted for a summary of different constitutive models.

Of all these models, the hyperbolic sine model illustrates the natural step of development from the potential law, as it allows the strain-rate range to be widened without introducing further parameters into the model. It represents an essentially phenomenological model which tries to replicate by means of an equation the behavior of the material collected on the S-curve.

Sellars in 1966 [12] proposed a constitutive model for hot deformation where the strain rate is related to a hyperbolic sine function of the flow stress, where in addition the effect of temperature is introduced by an exponential term of the activation energy.

$$\dot{\varepsilon} = A(\sinh \alpha\sigma)^n e^{\left(-\frac{Q}{RT}\right)} \tag{5}$$

Materials Research Proceedings **32** (2023) 264-273 https://doi.org/10.21741/9781644902615-30

Lin in 1993 [13] proposed a similar model, excluding the exponential term, for creep including damage variables ω. Additionally, his model is extended to a multi-axial formulation by defining a potential dissipation energy hyperbolic cosine function.

$$\dot{\varepsilon} = A \sinh(B\sigma) f(\omega) \tag{6}$$

In 1997, Dunne [14] points out the need to move from the potential model to the hyperbolic sine model if the strain rate range of the constitutive model is to be extended. He also proposes the inclusion of a grain size evolution term.

$$\dot{\varepsilon} = \frac{\alpha}{d^{\gamma}} \sinh(\beta\sigma) \tag{7}$$

This same model is then used by Lin in 2001 [15] to characterize the titanium alloy Ti-6Al-4V with determination of constants by genetic algorithm. The microstructural part of this model was further developed in 2005 [9]. Zhang in 2004 [16] returned to Sellar's model and related the values of the exponential parameter to the α and *m* parameters. In 2006, Bonet [17] proposed a slight modification of the previous model where the exponential affects the hyperbolic sine function and not its argument.

$$\sigma = \sigma_o \left[\sinh^{-1}\left(\frac{\dot{\varepsilon}}{\dot{\varepsilon}_o}\right)\right]^m \tag{8}$$

More recently Yang in 2020 [18] and Mosleh in 2021 [19] have incorporated the hyperbolic sine model into more complex models where potential, exponential and hyperbolic sine laws are coupled to characterize the material over a wide range of strain rate. This leads to an increase in the required number of parameters and their subsequent determination.

$$\dot{\varepsilon} = A[\sinh(\alpha\sigma)]^{\eta} e^{\left(-\frac{Q}{RT}\right)} \tag{9}$$

The aim of this work is to carry out a comparative study of the different hyperbolic sine models historically proposed to describe the superplastic behavior over a wide strain rate range with a number of parameters equal to or less than three. More complex multifunctional models or models with a description of the evolution of the microstructure are discarded. In order to do so, a brief theoretical assessment of the models studied is first made. Then, from a series of tests on AZ31 magnesium alloy at 450 ºC, the parameters for each model are extracted. These values are introduced into the constitutive model of the material in a finite element code to computationally obtain the forming time. This value is then compared with the experimental values to verify the model.

Methodology

a) Theoretical framework. The different constitutive models previously presented are summarized in only three options. The terms relating to temperature are not taken into account, as single temperature tests are studied, and those relating to microstructural evolution are also omitted since, due to the characteristics of the method for extracting the behavior of the material [7], this parameter is implicitly included.

Materials Research Proceedings **32** (2023) 264-273 https://doi.org/10.21741/9781644902615-30

Thus, the models to be compared are:

$$\sigma = \sigma_o \left[\sinh^{-1}\left(\frac{\dot{\varepsilon}}{\dot{\varepsilon}_o}\right)\right]^{m^*} \tag{10}$$

$$\sigma = \sigma_o \sinh^{-1}\left(\left[\frac{\dot{\varepsilon}}{\dot{\varepsilon}_o}\right]^{m^*}\right) \tag{11}$$

$$\sigma = \sigma_o \sinh^{-1}\left(\frac{\dot{\varepsilon}}{\dot{\varepsilon}_o}\right) \tag{12}$$

The different models have been combined into only three constitutive equations (10), (11) and (12) including a stress-related parameter σ_o, a strain-rate-related parameter $\dot{\varepsilon}_o$, and a third exponential parameter m^*, where m^* is used to differentiate from the parameter used for the potential function (2) and which is well defined in (1). To obtain the relationship between *m** and the sensitivity index, the expression (11) can be changed to

$$\sinh\left(\frac{\sigma}{\sigma_o}\right) = \left[\frac{\dot{\varepsilon}}{\dot{\varepsilon}_o}\right]^{m^*} \tag{13}$$

Given that the Taylor expansion of the hyperbolic sine function is

$$\sinh(x) = x + \frac{x^3}{3!} + \frac{x^5}{5!} + \cdots \tag{14}$$

Equation (13) can be simplified for small stress values as

$$\sinh\left(\frac{\sigma}{\sigma_o}\right) \cong \frac{\sigma}{\sigma_o} = \left[\frac{\dot{\varepsilon}}{\dot{\varepsilon}_o}\right]^{m^*} \tag{15}$$

arriving at the same potential function with value $K = {\sigma_o}/{\dot{\varepsilon}_o^{m^*}}$. Therefore, it can be concluded that $m^* = m$ when $\sigma \to 0$. In other words, m^* is the slope of the hyperbolic sine function for low stress values and can be then related to the sensitivity index. This same development can be followed with identical result for (10).

b) Experimental procedure. Experimental tests were carried out on disc specimens on a cylindrical mold of 22.5 mm radius and 3 mm entry radius. The sheets, with an initial thickness of 0.75 mm, were preheated at 450 ºC and subjected to 0.2, 0.25, 0.35, 0.5 and 0.75 MPa constant pressure [7,20], Table 1. The output variable to be studied is the evolution of the height at the central point and specifically the time when the height equals the mold radius. A final dome configuration is expected at this point. Forming time experimental values are included in Table 1 together with the values of *K* and *m*. A progressive decrease of *m* is observed as higher strain-rate values are reached.

Materials Research Proceedings **32** (2023) 264-273 https://doi.org/10.21741/9781644902615-30

Table 1. Summary table of trials including estimative values of K and m

External Pressure [MPa]	*Forming time [s]*	$K\ [MPa \cdot s^m]$	m
0.2	3403	565.2	0.544
0.25	2435	565.2	0.544
0.35	1185	565.2	0.544
0.5	423	171.2	0.391
0.75	87	70.6	0.267

With these five tests and following the methodology described in [7], five corresponding values of stress and strain rate are obtained to characterize the material by plotting the hyperbolic sine law that best match the material behavior. Higher pressure from [20] were neglected from the study since they are relative fast processes where transient periods are important and the aforementioned method is less accurate. Using the *Matlab* [21] curve-fitting application, the following parameter values are obtained for the hyperbolic sine models, where the R^2 value is attached, Table 2. Fig. 2 shows how these three models adjust to experimental values of stress and strain-rate.

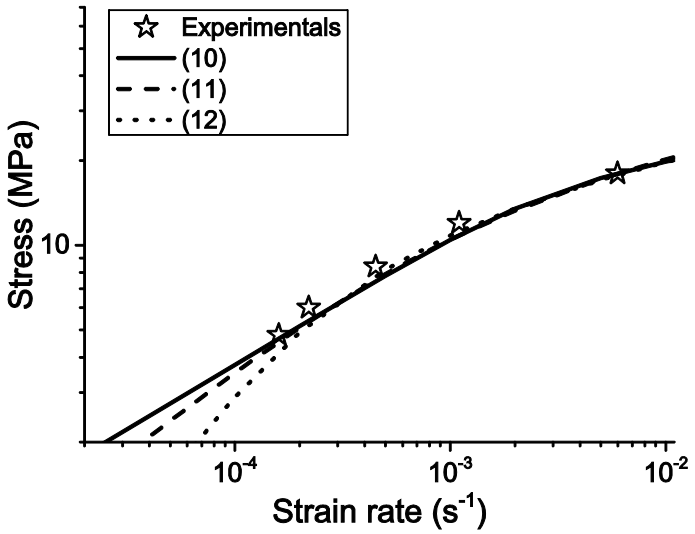

Fig 2. Adjustment of hyperbolic sine models to experimental values

Table 2. Numerical values for the three models' parameters

Model	$\sigma_o\ [MPa]$	$\dot{\varepsilon}_o\ [s^{-1}]$	$m*$	R^2
(10)	12.72	0.00144	0.4567	0.998
(11)	7.416	0.00033	0.5932	0.999
(12)	3.872	0.00012		0.996

The reason for using a hyperbolic sine function is illustrated in Fig. 2, in order to accommodate processes with a wide strain-rate range, from ~10^{-4} to ~10^{-2}. For narrower ranges, e.g. those obtained for [0.2-0.5] MPa, the hyperbolic sine closely matches a typical potential function and its results, so its use is less justified.

c) FEM simulations. The three hyperbolic sine models are then tested under *Marc Mentat* FE code using an axisymmetric finite element model, with constant pressure and static analysis, considering that the dynamic effects are negligible [22], and with a termination criterion when the central node is displaced by 22.5 mm. 0.25 mm length quadratic elements are used through the blank thickness.

Finally, the material model is added externally by means of a simple Fortran routine. Fig. 3 depicts an example of the strain-rate evolution during five simulation times for 0.5 MPa.

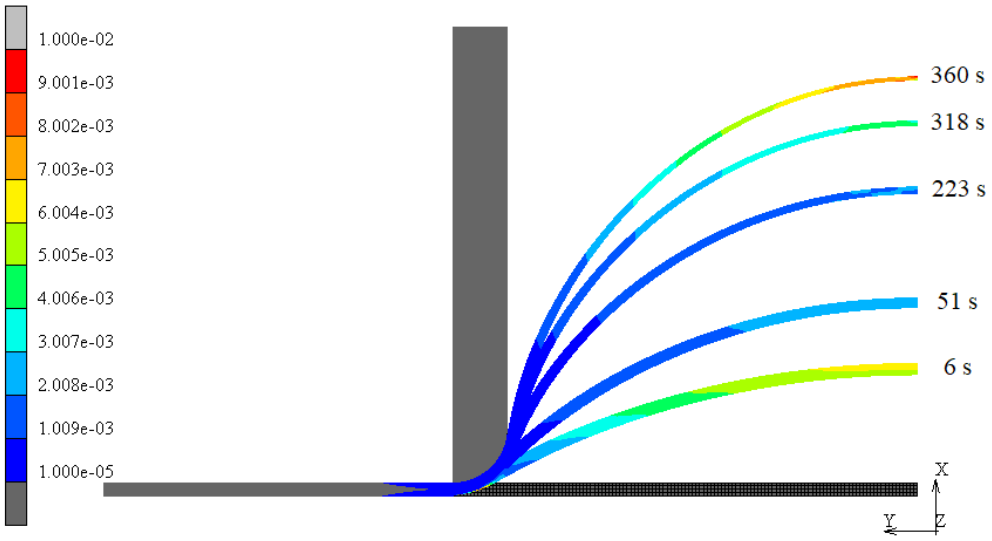

Fig. 3. Strain-rate evolution at five stages during a 0.5 MPa test

Results and Discussions

Table 3 shows the comparative results, for the five pressure values, between the experimental forming time and the three computational forming times using models (10), (11) and (12) together with the parameters in Table 2.

Table 3. Forming time results

External Pressure [MPa]	*Forming Time [s]*			
	Experimental	(10)	(11)	(12)
0.2	3403	3035	3226	2776
0.25	2435	1835	2051	1900
0.35	1185	828	865	914
0.5	423	296	201	295
0.75	87	37	11	44

These values are shown graphically in Fig. 4. A number of remarks can be drawn from these results:

- None of the three models performs significantly better than the others. Even the 2-parameter model presents time estimations of the same order as the models where the exponent term is included.
- The relative deviation from the experimental values shows a positive trend as the external pressure increases.
- All three models present an underestimation of the forming time, i.e. they predict a lower time than the real one. This may be due, as shown in Fig. 2, to the fact that all three models predict a higher strain rate for the reference stress values for the five tests.

Materials Research Proceedings **32** (2023) 264-273 https://doi.org/10.21741/9781644902615-30

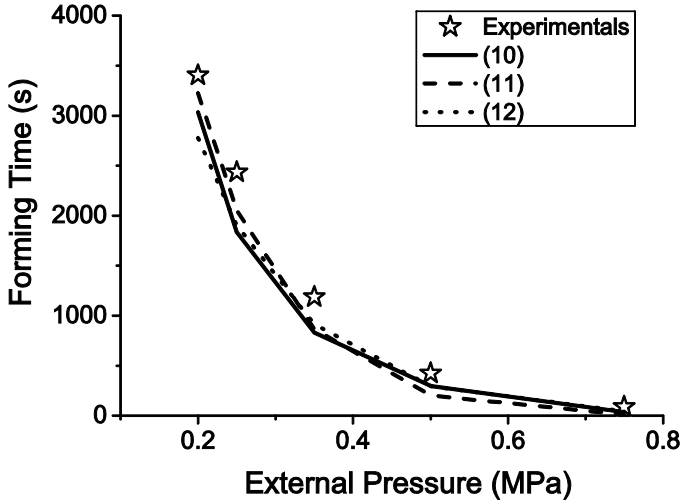

Fig. 4. Forming time versus external pressure

On this last observation, it should be added that this behavior is mainly seen in the pressure range from 0.2 to 0.5 MPa, Fig. 5. However, for the 0.75 MPa test, a sudden softening in the final stage of forming must be included, Fig. 6. This unexpected behavior can also be seen in Fig. 7 where the final shape is compared for pressures of 0.5 and 0.75 MPa. For the latter test, the final shape departs from a dome pattern.

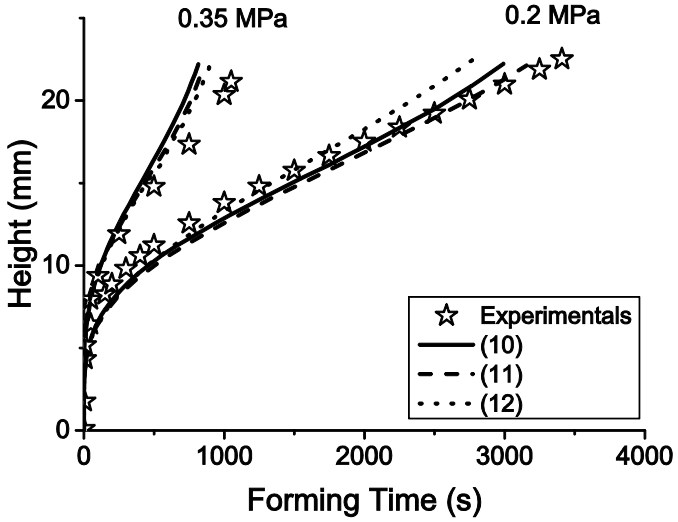

Fig. 5. Center sample height evolution for 0.2 and 0.35 MPa

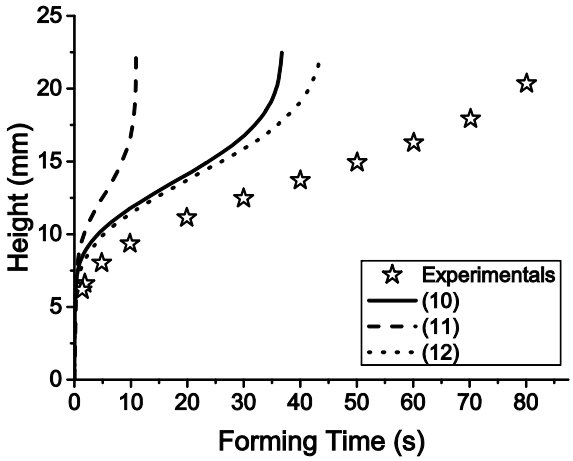

Fig. 6. Center sample height evolution for 0.75 MPa

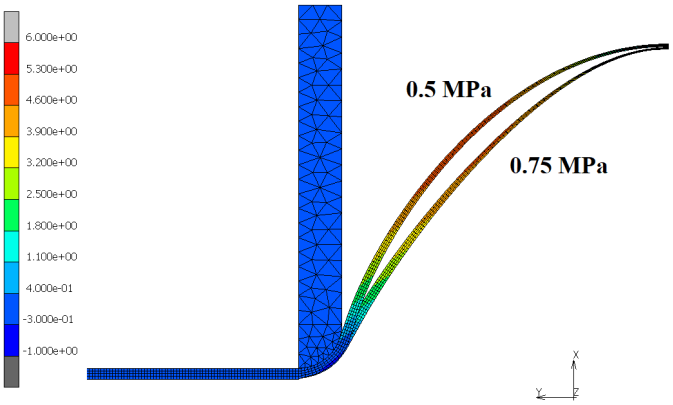

Fig 7. Final configuration for tests at 0.5 and 0.75 MPa. The color scheme represents the horizontal displacements.

Conclusions

In view of the results obtained following the methodology described above, the next conclusions can be drawn:

- The three proposed models give similar results. In other words, the inclusion of a third parameter in the form of an exponent does not provide significant improvements.
- In case such an exponent is used, it seems desirable to avoid confusion with the sensitivity index *m*, with a different nomenclature, since, as previously developed, its relationship is limited to stress values tending to 0, where SPF processes are not common.
- All three models overestimate the strain-rate values over the flow stress. It seems necessary to corroborate whether this trend is repeated for other materials in future work.
- The values of forming time obtained computationally present a first estimation with values in the order of the experimental time with errors ranging from 10% to 50%. It is also observed that these values increase progressively as the external pressure increases.
- It seems also necessary, in future work, to study if the inclusion of an additional parameter allows correcting this overestimation of the strain rate in order to improve the model.

- For higher strain rate values, i.e., approximately 10^{-2} s^{-1} and an approximate forming time of 100 s, anomalous behavior is observed in the FEM model, which requires a separate study to correct the finite element model and achieve more stable behavior for larger strain-rate ranges.

References

[1] I.C. And, R.S. Mishra, Materials Processing Handbook, Taylor & Francis Group, 2007.

[2] E. Alabort, D. Putman, R.C. Reed, Superplasticity in Ti-6Al-4V: Characterisation, modelling and applications, Acta Mater., 95 (2015) 428-442. https://doi.org/10.1016/j.actamat.2015.04.056

[3] T. Yasmeen, Z. Shao, L. Zhao, P. Gao, J. Lin, J. Jiang, Constitutive modeling for the simulation of the superplastic forming of TA15 titanium alloy, Int. J. Mech. Sci., 164 (2019). https://doi.org/10.1016/j.ijmecsci.2019.105178

[4] W. Zhou, J. Lin, D.S. Balint, T.A. Dean, Clarification of the effect of temperature and strain rate on workpiece deformation behaviour in metal forming processes, Int. J. Mach. Tools Manuf., 171 (2021) 103815. https://doi.org/10.1016/j.ijmachtools.2021.103815

[5] P.N. Comley, ASTM E2448-A Unified Test for Determining SPF Properties, J. Mater. Eng. Perform., 17 (2008) 183-186. https://doi.org/10.1007/s11665-007-9181-5

[6] G.C. Cornfield, R.H. Johnson, The forming of superplastic sheet metal, Int. J. Mech. Sci., 12 (1970) 479-490. https://doi.org/10.1016/0020-7403(70)90075-5

[7] L. García-Barrachina, D. Sorgente, L. Tricarico, A.J. Gámez, A method for estimating superplastic material parameters via free-inflation tests, J. Mater. Res. Technol., 11 (2021) 1387-1395. https://doi.org/10.1016/j.jmrt.2021.01.116

[8] N. Chandra, Constitutive behaviour of superplastic materials, Int. J. Non. Linear. Mech., 37 (2002) 461-484. https://doi.org/10.1016/S0020-7462(01)00021-X

[9] J. Lin, T.A. Dean, Modelling of microstructure evolution in hot forming using unified constitutive equations, J. Mater. Process. Technol., 167 (2005) 354-362. https://doi.org/10.1016/j.jmatprotec.2005.06.026

[10] A.J. Carpenter, A.R. Antoniswamy, J.T. Carter, L.G. Hector, E.M. Taleff, A mechanism-dependent material model for the effects of grain growth and anisotropy on plastic deformation of magnesium alloy AZ31 sheet at 450 C, Acta Mater., 68 (2014) 254-266. https://doi.org/10.1016/j.actamat.2014.01.043

[11] O. Majidi, M. Jahazi, N. Bombardier, A viscoplastic model based on a variable strain rate sensitivity index for superplastic sheet metals, Int. J. Mater. Form., 12 (2019) 693-702. https://doi.org/10.1007/s12289-018-1443-2

[12] C.M. Sellars, W.J. McTegart, On the mechanism of hot deformation, Acta Metall., 14 (1966) 1136-1138. https://doi.org/10.1016/0001-6160(66)90207-0

[13] H.D.R. Lin J., D. B.F., A new design of uniaxial testpiece with slit extensometer ridges for improved accuracy of strain measurement, Int. J. Mech. Sci., 35 (1993) 63-78. https://doi.org/10.1016/0020-7403(93)90065-3

[14] T.W. Kim, F.P.E. Dünne, Determination of superplastic constitutive equations and strain rate sensitivities for aerospace alloys, Proc. Inst. Mech. Eng. Part G J. Aerosp. Eng., 211 (1997) 367-380. https://doi.org/10.1243/0954410971532730

[15] J. Lin, Selection of material models for predicting necking in superplastic forming, Int. J. Plast., 19 (2002) 469-481. https://doi.org/10.1016/S0749-6419(01)00059-6

[16] B. Zhang, D.J. Mynors, A. Mugarra, K. Ostolaza, Representing the superplasticity of Inconel 718, J. Mater. Process. Technol., 153-154 (2004) 694-698. https://doi.org/10.1016/j.jmatprotec.2004.04.138

[17] J. Bonet, A. Gil, R.D.R.D. Wood, R. Said, R. V Curtis, Simulating superplastic forming, Comput. Methods Appl. Mech. Eng., 195 (2006) 6580-6603. https://doi.org/10.1016/j.cma.2005.03.012

[18] J. Yang, J. Wu, Q. Zhang, R. Han, K. Wang, The simple hyperbolic-sine equation for superplastic deformation and parameters optimization, J. Mater. Res. Technol., 9 (2020) 10819-10829. https://doi.org/10.1016/j.jmrt.2020.07.076

[19] A.O. Mosleh, A.D. Kotov, A.A. Kishchik, O. V. Rofman, A. V. Mikhaylovskaya, Characterization of superplastic deformation behavior for a novel al-mg-fe-ni-zr-sc-based alloy: Arrhenius-based modeling and artificial neural network approach, Appl. Sci., 11 (2021) 1-18. https://doi.org/10.3390/app11052208

[20] D. Sorgente, G. Palumbo, L.D. Scintilla, L. Tricarico, Gas forming of an AZ31 magnesium alloy at elevated strain rates, Int. J. Adv. Manuf. Technol., 83 (2016) 861-872. https://doi.org/10.1007/s00170-015-7614-0

[21] The MathWorks Inc., MATLAB Version: 9901592791 (R2020b), (2020).

[22] L. García-Barrachina, A.J. Gámez, A forming time estimator of superplastic free bulge tests based on dimensional analysis, Int. J. Mater. Form., 14 (2021) 499-506. https://doi.org/10.1007/s12289-019-01527-x